AD NUMBER
AD466351
LIMITATION CHANGES
TO: **Approved for public release; distribution is unlimited.**
FROM: **Distribution authorized to U.S. Gov't. agencies and their contractors; Administrative/Operational Use; 25 FEB 1965. Other requests shall be referred to Defense Advanced Research Projects Agency, 675 North Randolph Street, Arlington, VA 22203-2114.**
AUTHORITY
ARPA ltr, 6 Nov 1972

X-RAY TRANSPORT - I

(SCATTERING)

KN-65-62(R)

25 February 1965

Kaman Nuclear
COLORADO SPRINGS, COLORADO
A DIVISION OF KAMAN AIRCRAFT CORPORATION

Kaman Nuclear
A DIVISION OF KAMAN AIRCRAFT CORPORATION
GARDEN OF THE GODS RD., COLORADO SPRINGS, COLO.

X-RAY TRANSPORT - I

(SCATTERING)

KN-65-62(R) 25 February 1965

Wm. J. Veigele

SUBMITTED TO: Advanced Research Projects Agency
Order Number 343-62
Project Code Number 7200
Contract SD-135

F O R E W O R D

As the temperature of thermal sources is increased, a region ($kT > 2$ kev) is encountered in which transport of the emitted photons (of the order of 10 - 500 kev) through low and medium atomic number materials is determined by other than photoelectric absorption only. Recent Kaman Nuclear reports include pertinent discussions, but it was considered useful to generalize and extend this work and to collect working equations and graphs under one cover. This paper briefly discusses the phenomenology of Compton and Rayleigh scattering, establishes working equations, provides tables of scattering data, displays graphs of equations and data in the photon energy range from one to one-thousand kev, discusses the effect of scattering on x-ray transport, and suggests general methods of solution of the multiple scattering problem.

A B S T R A C T

Compton and Rayleigh scattering for x-rays in the range of 10 to 1000 kev is described, and equations, data, and graphs are presented. Effects of scattering on transport are discussed, and methods of solving the multiple scattering transport problem are suggested.

LIST OF SYMBOLS

E	recoil electron kinetic energy
h	Planck's constant
B_e	electron binding energy
θ	angle between incident and scattered photon directions
φ	angle between incident photon and recoil electron
m_o	electron rest mass
c	speed of light
λ_o	incident photon wavelength
λ'	scattered photon wavelength
ν_o	incident photon frequency
ν'	scattered photon frequency
α	$h\nu_o/m_oc^2$
α'	$h\nu'/m_oc^2$
$d({}_e\sigma)$	differential collision cross section per electron
$d({}_e\sigma_s)$	differential scattering cross section per electron
$d({}_e\sigma_a)$	differential absorption cross section per electron
$d({}_a\sigma)$	differential collision cross section per atom
$d({}_a\sigma_s)$	differential scattering cross section per atom
$d({}_a\sigma_a)$	differential absorption cross section per atom
θ_ℓ	lower limit for θ
θ_u	upper limit for θ
${}_e\sigma$	total (average) collision cross section per electron

LIST OF SYMBOLS (Continued)

$_{e}\sigma_{s}$	total (average) scattering cross section per electron
$_{e}\sigma_{a}$	total (average) absorption cross section per electron
$_{a}\sigma$	total (average) collision cross section per atom
$_{a}\sigma_{s}$	total (average) scattering cross section per atom
$_{a}\sigma_{a}$	total (average) absorption cross section per atom
$d(_{e}\sigma_{incoh})$	differential incoherent collision cross section per electron
S	incoherent scattering function
v	incoherent scattering function parameter
F	coherent atomic structure factor
u	coherent atomic structure factor parameter
$d(_{a}\sigma_{coh})$	differential coherent scattering cross section per atom
B	build-up factor
a_{o}	Bohr radius = $h^2/4\pi^2me^2$
e	electronic charge
ρ	material density
d	material dimension

LIST OF FIGURES

LIST OF TABLES

TABLE OF CONTENTS

X-RAY TRANSPORT - I
(SCATTERING)

1. Introduction

In the transport of x-rays through matter, there are three dominant mechanisms of interaction. These are the photoelectric effect, the Compton effect, and pair production, having domains of relative dominance[1] as shown in Figure 1.

The region of interest here is $10 < h\nu_o < 1000$ kev where pair production may be neglected. Other less dominant effects have been shown to be unimportant[2] except for the Rayleigh effect which will be considered below. Also, the Compton effect[3] is discussed in terms of its three components: (1) absorption, (2) inelastic scattering from free electrons, and (3) inelastic scattering from bound electrons.

2. Compton Free Electron Inelastic Scattering Relationships

Assuming a stationary electron, the recoil electron kinetic energy E greater than the electron binding energy B_e, and applying the laws of conservation of relativistic energy and momentum to the situation in Figure 2.

One obtains for the scattered photon wavelength shift

$$\lambda' - \lambda_o = (h/m_o c)\ (1 - \cos\theta) \qquad (1)$$

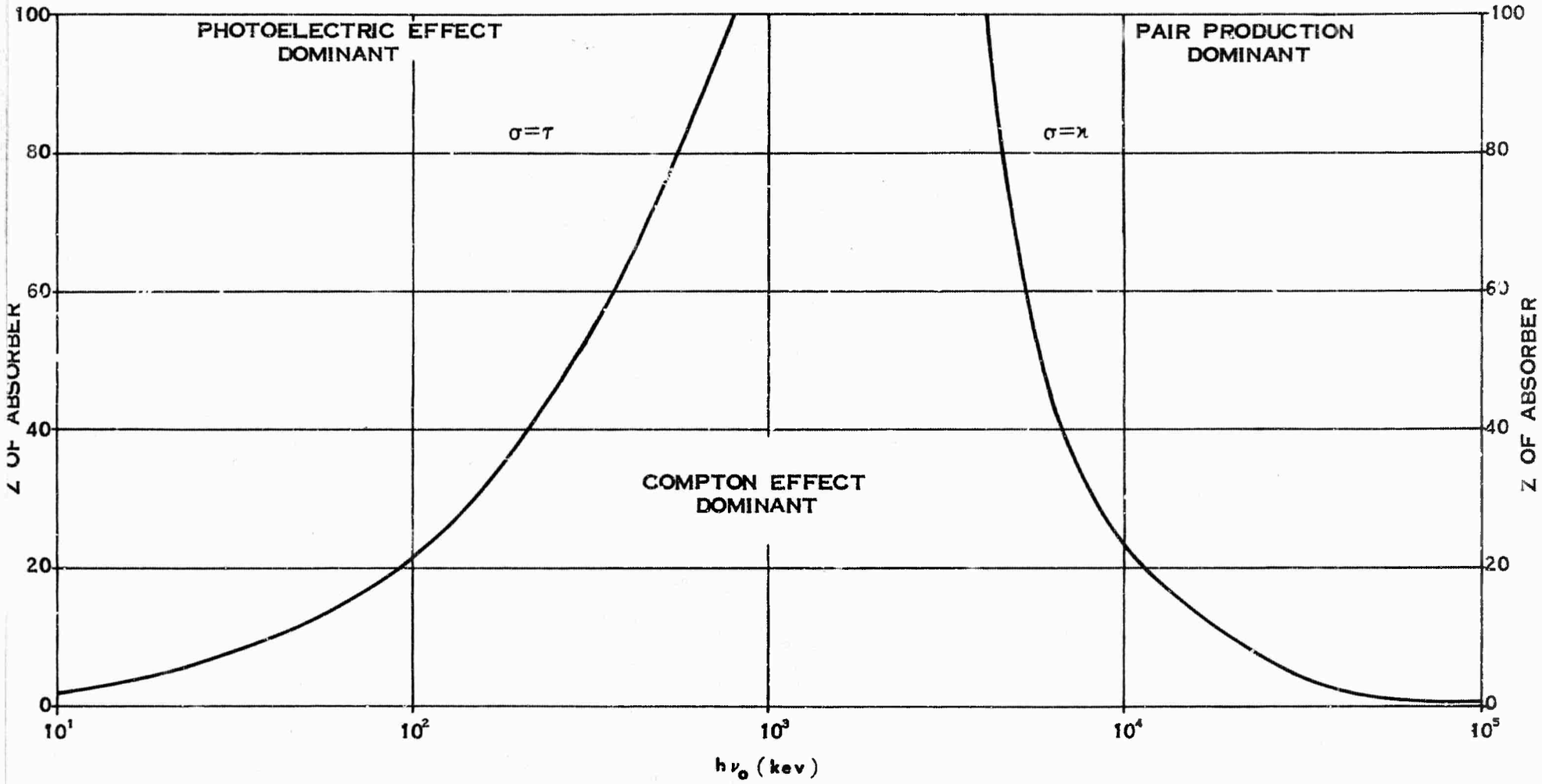

FIGURE 1

DOMAINS OF DOMINANCE OF γ - RAY ATTENUATION MECHANISMS

COMPTON SCATTERING

(FREE ELECTRON – INCOHERENT)

$$\lambda' - \lambda_o = (h/m_o c)\,(1 - \cos\theta)$$

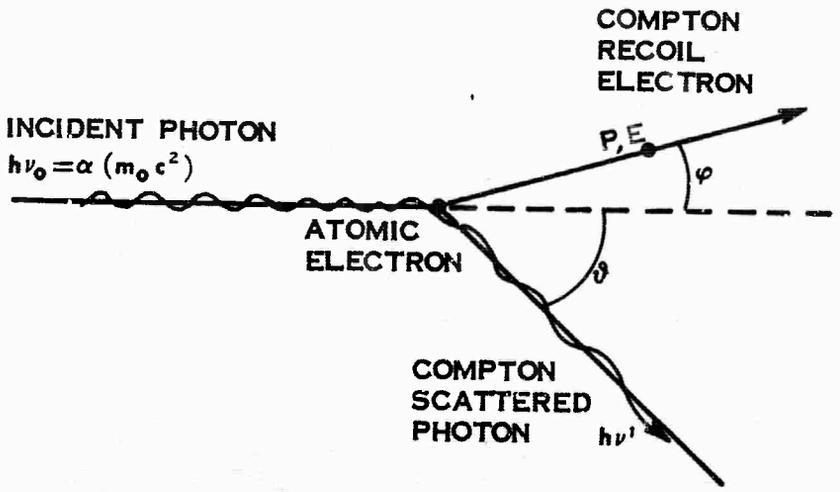

FIGURE 2

COMPTON SCATTERING OF A PHOTON BY AN ELECTRON

and for the scattered photon energy, using $\alpha = h\nu_o/m_o c^2$,

$$h\nu' = h\nu_o[1 + \alpha(1 - \cos\theta)]^{-1} \qquad (2)$$

which is plotted in Figure 3 for $10 < h\nu_o < 1000$ kev. Equation 2 determines the energy $h\nu'$ of a photon of incident energy $h\nu_o$ scattered at an angle θ.

The recoil electron direction, φ, is related to θ and α by

$$\cot\varphi = (1 + \alpha)\tan(\theta / 2) \qquad (3)$$

which is shown in Figure 4.

Recoil electron kinetic energy is given by

$$E = h\nu_o - h\nu' = h\nu_o\alpha(1 - \cos\theta) / [1 + \alpha(1 - \cos\theta)] \qquad (4)$$

and is plotted in Figure 5. This may be expressed in terms of φ using Equation (3).

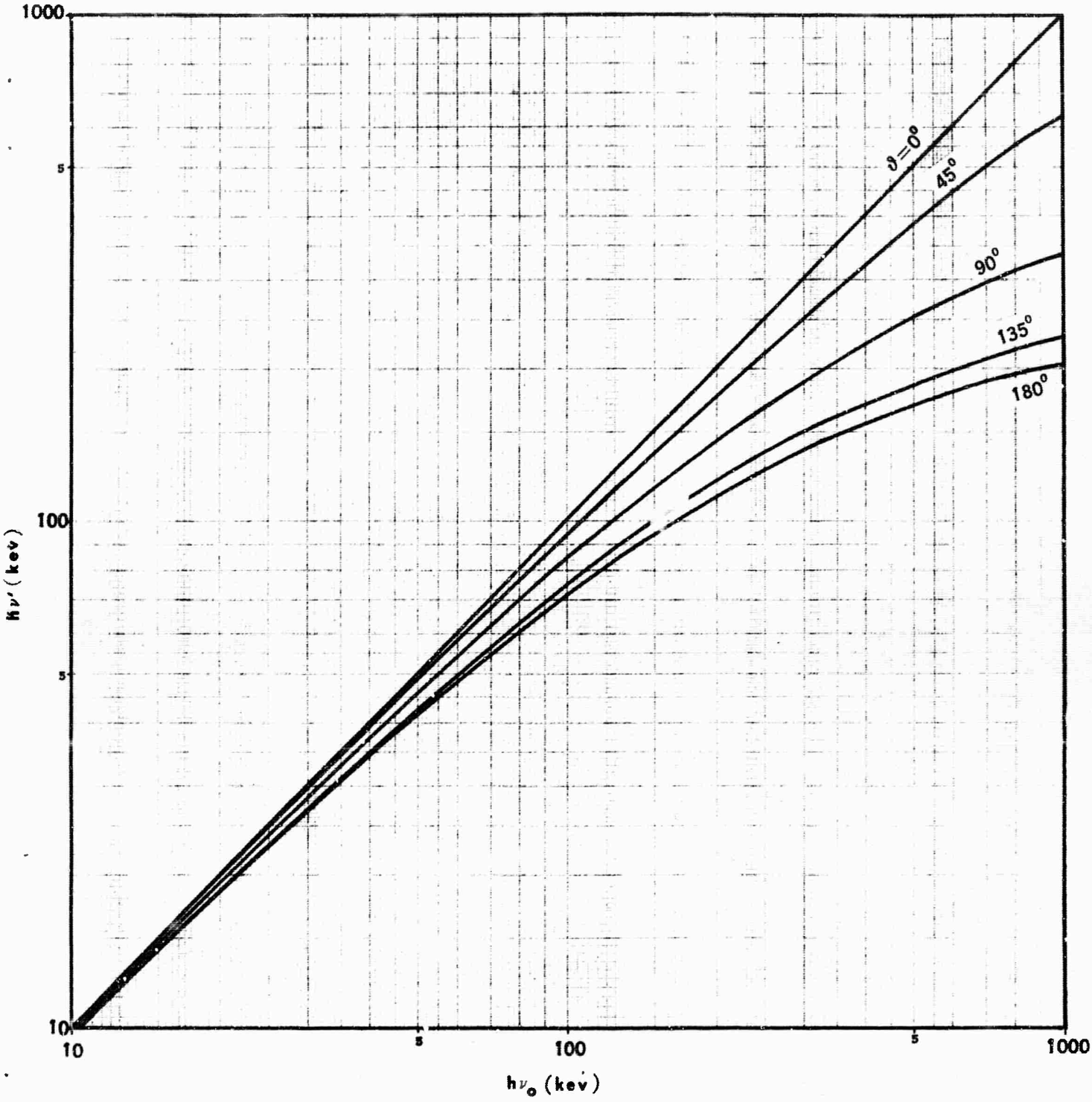

FIGURE 3

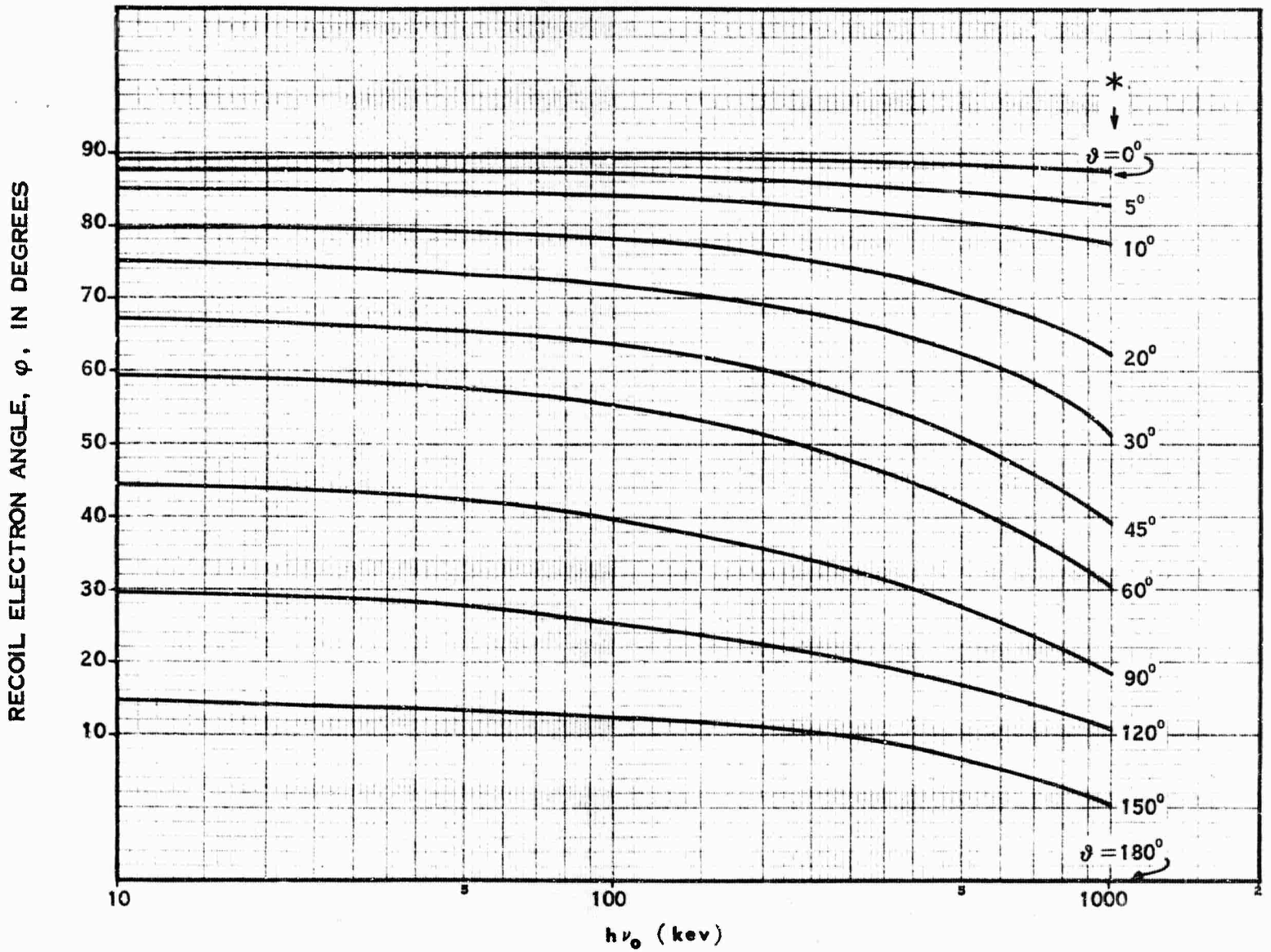
RECOIL ELECTRON ANGLE, φ, IN DEGREES
90
80
70
60
50
40
30
20
10
10
5
100
5
1000
2
hν₀ (kev)
*
ϑ=0°
5°
10°
20°
30°
45°
60°
90°
120°
150°
ϑ=180°

FIGURE 4

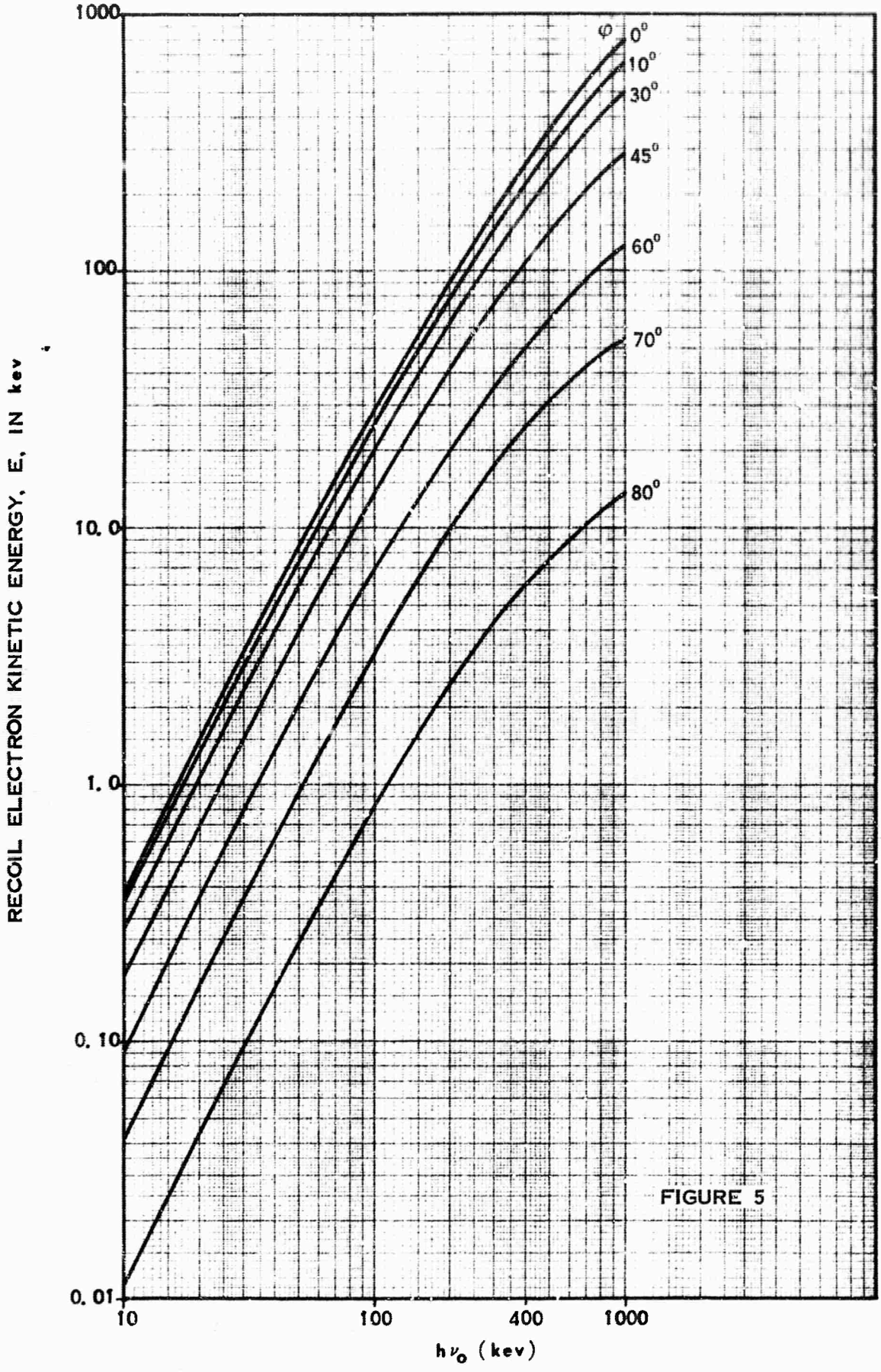
1000
100
10. 0
1. 0
0. 10
0. 01
10
100
400
1000
φ
0°
10°
30°
45°
60°
70°
80°
RECOIL ELECTRON KINETIC ENERGY, E, IN kev
hν₀ (kev)

FIGURE 5

3. Compton Free Electron Inelastic Scattering Cross Sections

When photons collide with electrons, the number of photons scattered in a particular direction may be described by a differential scattering cross section per electron

$$d({}_p\sigma) = \frac{\text{number scattered (number/sec-electron)}}{\text{incident (number/cm}^2 \text{ - sec)}}. \qquad (5)$$

The amount of energy scattered in a particular direction may be given by a differential scattering cross section per electron

$$d({}_e\sigma_s) = \frac{\text{energy scattered/sec (erg/sec-electron)}}{\text{incident intensity (erg/cm}^2\text{-sec)}}, \qquad (6)$$

and the amount of energy absorbed by the electron may be given by the differential absorption cross section per electron

$$d({}_e\sigma_a) = \frac{\text{energy absorbed/sec (erg/sec-electron)}}{\text{incident intensity (erg/cm}^2\text{-sec)}}. \qquad (7)$$

These are related as follows [and shown in Figure (6)]:

$$d({}_e\sigma) = d({}_e\sigma_s) + d({}_e\sigma_a) , \qquad (8)$$

$$d({}_e\sigma_s) = \frac{\nu'}{\nu_o}\, d({}_e\sigma) , \qquad (9)$$

and

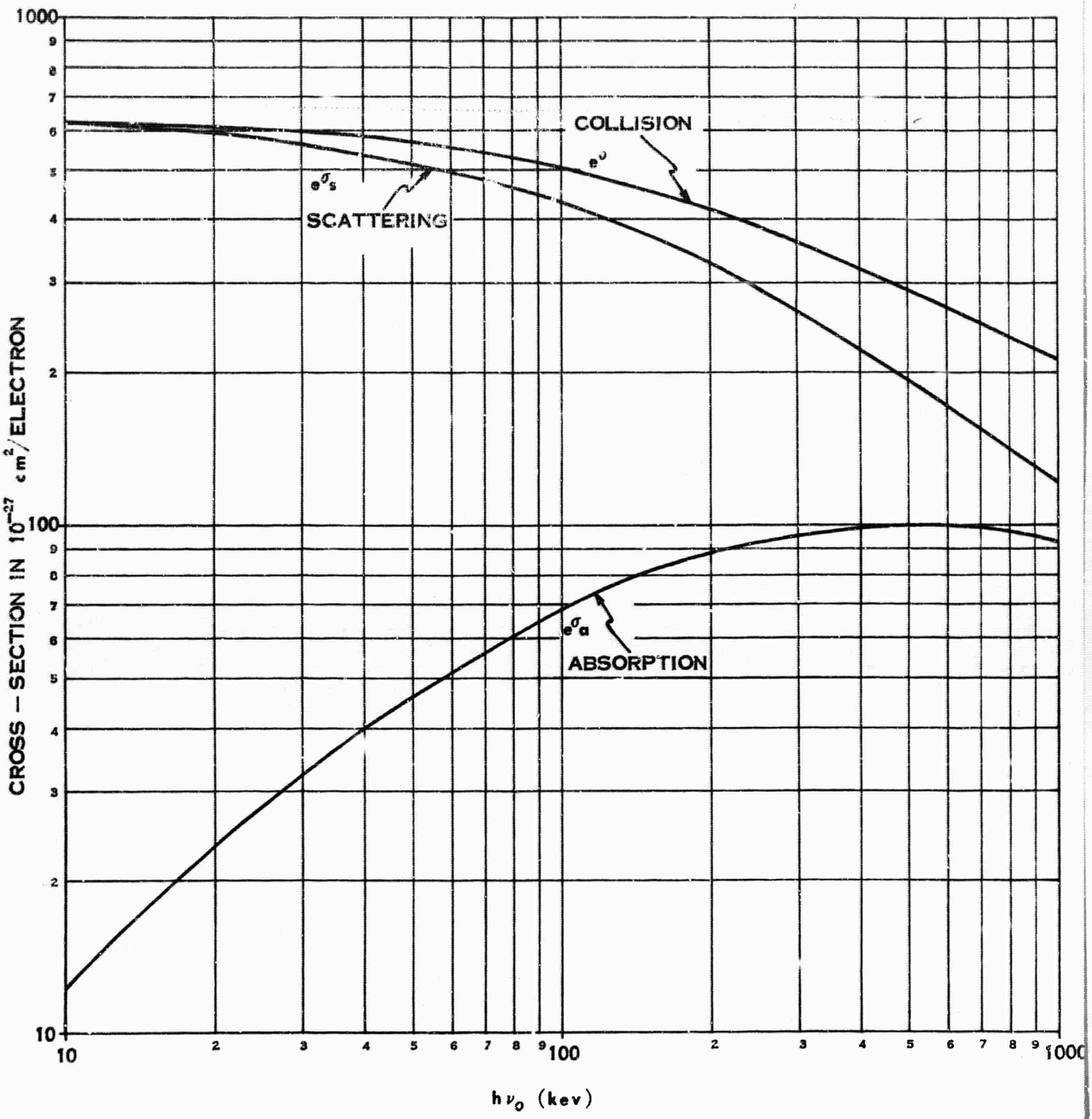

FIGURE 6

KLEIN – NISHINA CROSS SECTIONS,
DEPENDENCE ON INCIDENT ENERGY

$$d({}_e\sigma_a) = \frac{\nu_o - \nu'}{\nu_o}\, d({}_e\sigma) = \frac{\nu_o - \nu'}{\nu'}\, d({}_e\sigma_s). \qquad (10)$$

The differential cross sections per atom are obtained by multiplying by the atomic number Z of the material, e.g.,

$$d({}_a\sigma) = Z\, d({}_e\sigma)\ . \qquad (11)$$

Explicitly, the differential collision cross section for incident unpolarized radiation derived by Klein and Nishina[4] is given by

$$d({}_e\sigma) = r_o^2\, d\Omega \left\{ 1/[1 + \alpha(1 - \cos\theta)]^2 \right\} [(1 + \cos^2\theta)/2]$$

$$[1 + \left\{ \alpha^2(1 - \cos^2\theta)^2/(1 + \cos^2\theta)\, [1 + \alpha(1 - \cos\theta)] \right\}] \qquad (12)$$

where $r_o = e^2/m_o c^2 = 2.818 \times 10^{-13}$ cm and $d\Omega$ = differential element of solid angle at θ into which photons are scattered. This equation is known to agree well with experiments up to $\alpha \cong 600$. For small α it reduces to the Thomson scattering equation. From Equations (8), (9), (10), and (11), one may obtain explicit forms for $d({}_e\sigma_s)$, $d({}_e\sigma_a)$, $d({}_a\sigma_s)$, and $d({}_a\sigma_a)$. From

$$d\Omega = 2\pi \sin\theta\, d\theta \qquad (13)$$

we have

$$d({}_e\sigma) \,/\, d\theta = 2\pi \sin\theta \; d({}_e\sigma) \,/\, d\Omega, \qquad (14)$$

which gives the probability per incident photon per electron per cm^2 of material that the scattered photon will be directed between θ and $\theta + d\theta$. This is shown in Figure 7.

Using Equations (3) and (13), the number of electrons recoiled into $d\varphi$ at φ may be written

$$d({}_e\sigma)/d\varphi = [d({}_e\sigma)/d\Omega]\,[2\pi(1 + \cos\theta)\sin\varphi] \,/\, (1 + \alpha)\sin^2\varphi. \qquad (15)$$

Cross sections giving the probability of an event occurring so that a photon is scattered into a restricted angular region may be determined from the integrals of the differential cross sections; e.g.,

$$e\sigma\,(\theta_\ell \le \theta \le \theta_u) = \int_{\theta_\ell}^{\theta_u} [d({}_e\sigma) \,/\, d\Omega]\, d\Omega. \qquad (16)$$

Values[1] for $(0 \le \theta \le \theta_u)$ are plotted in Figure 8, from which much useful information may be obtained, such as:

(1) the number of photons scattered into the interval $\theta_1 \le \theta \le \theta_2$ corresponds to ${}_e\sigma(\theta_2) - {}_e\sigma(\theta_1)$,

(2) the collision cross section for forward scattering is ${}_e\sigma(\le \pi / 2)$ and for backward scattering is ${}_e\sigma(\le\pi) - {}_e\sigma(\le\pi/2)$,

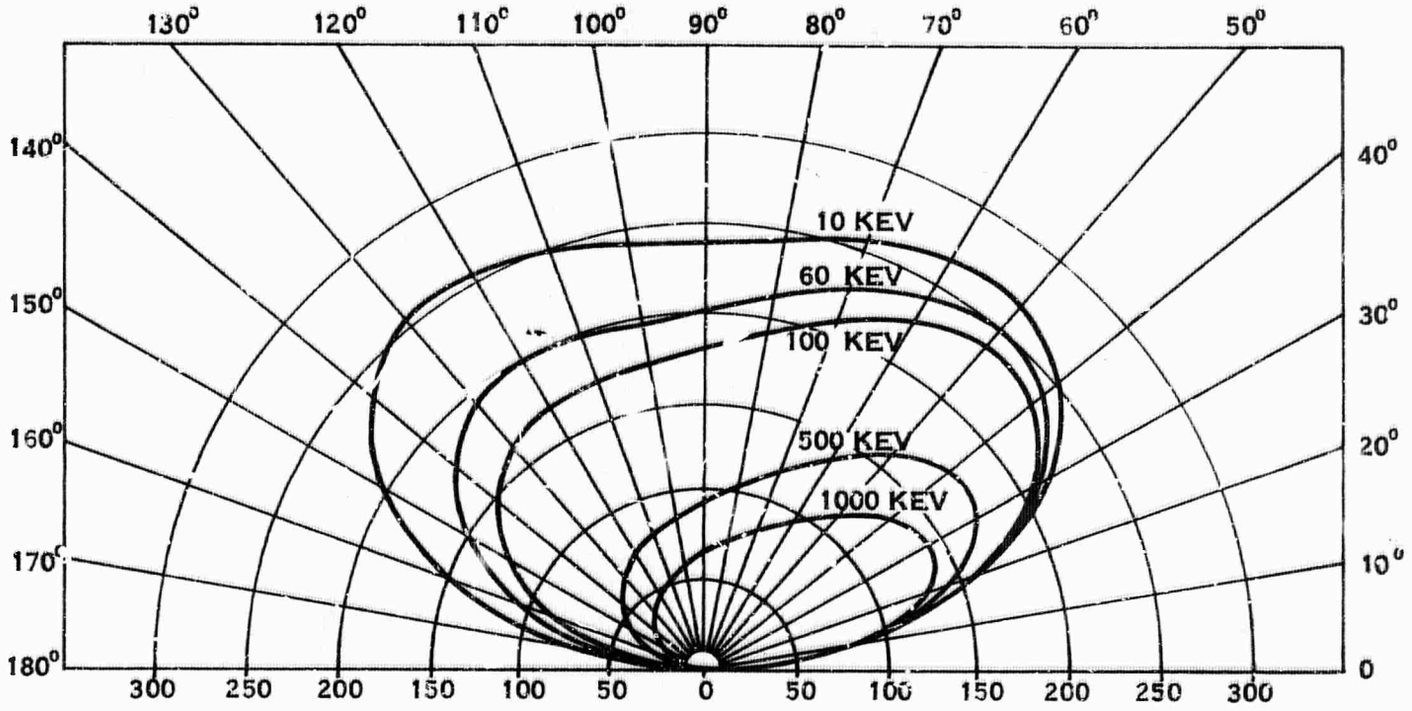
130°
120°
110°
100°
90°
80°
70°
60°
50°
140°
150°
160°
170°
180°
40°
30°
20°
10°
0
10 KEV
60 KEV
100 KEV
500 KEV
1000 KEV
300
250
200
150
100
50
0
50
100
150
200
250
300
$\frac{d(e\sigma)}{d\vartheta}$ IN 10^{-27} CM^2/RADIAN – ELECTRON

FIGURE 7

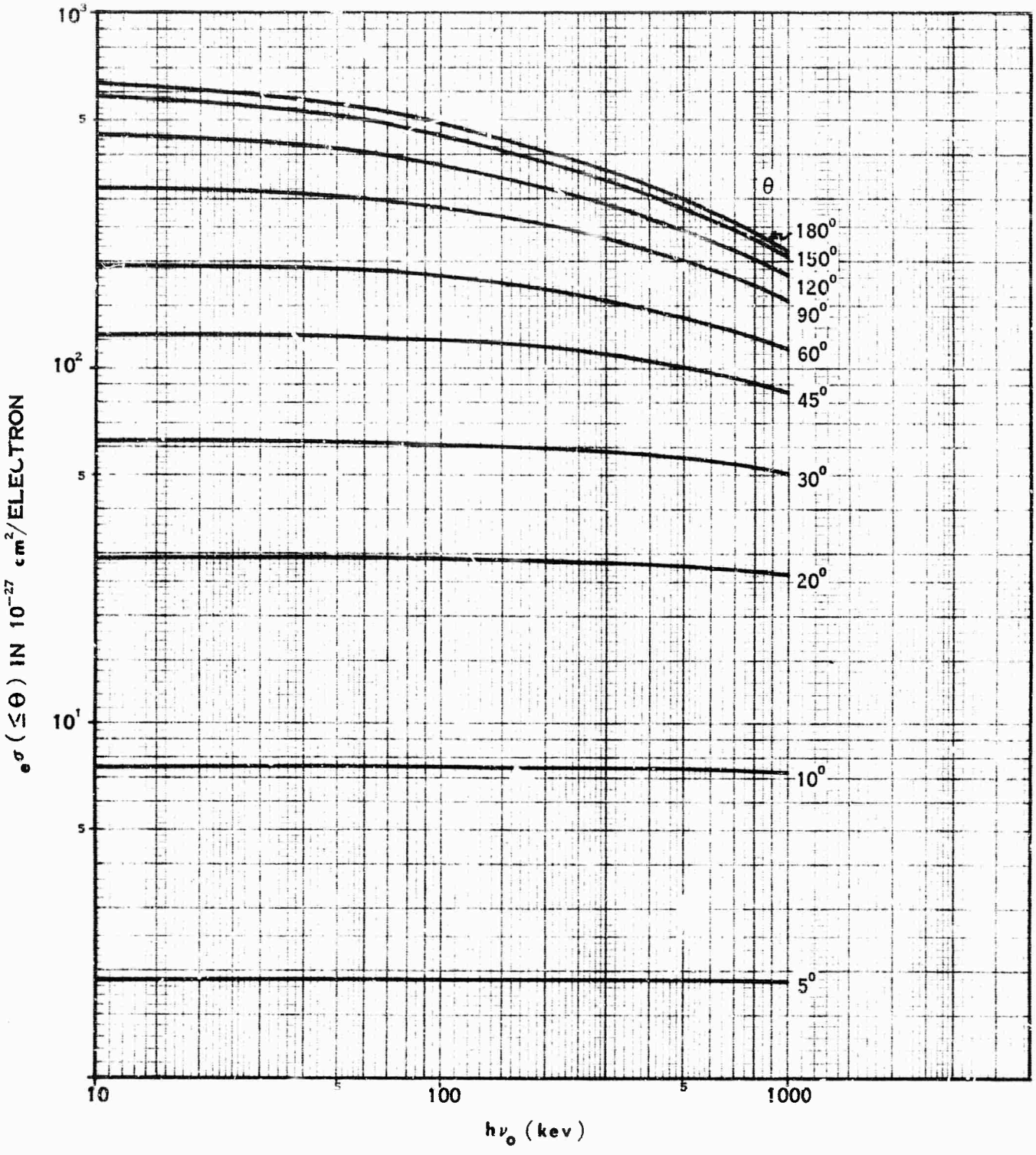
10^3
5
10^2
5
10^1
5
$_e\sigma$ ($\leq\theta$) IN 10^{-27} cm^2/ELECTRON
θ
180°
150°
120°
90°
60°
45°
30°
20°
10°
5°
10
5
100
5
1000
$h\nu_o$ (kev)

FIGURE 8

(3) the number of recoil electrons scattered into $\varphi_1 \leq \varphi \leq \varphi_2$ is read from Figure 8 after using Equation (3), or Figure 4,

(4) the number of photons scattered between θ_1 and θ_2 is the number of electrons scattered between φ_1 and φ_2 where the angles are related by Equation (3), and

(5) the fraction of scattered photons with more than an arbitrary energy is obtained in conjunction with Figure 3. For example, what fraction of 100 kev photons have energy greater than 80 kev? From Figure 3, $\theta \leq 100^\circ$; and from Figure 8, ${}_e\sigma(\leq 100^\circ) = 320$ and ${}_e\sigma(\leq 180^\circ) = 500$; thus, the fraction is $320/500 = .64$.

One also may obtain, from Equation (16), the average (total over-all scattering angles) collision cross section per electron, which is the probability of removal of a photon from a collimated beam while passing through an absorber with one electron/cm^2,

$$ {}_e\sigma = \int_0^\pi d({}_e\sigma) $$

$$ = 2\pi r_o^2 \left\{ \frac{1+\alpha}{\alpha^2} \left[\frac{2(1+\alpha)}{1+2\alpha} - \frac{\ln(1+2\alpha)}{\alpha} \right] + \frac{\ln(1+2\alpha)}{2\alpha} - \frac{(1+3\alpha)}{(1+2\alpha)^2} \right\} \quad (17) $$

which, for $\alpha \ll 1$ becomes

$$ {}_e\sigma \cong (8\pi r_o^2/3)\left[1 - 2\alpha + (26\alpha^2/5) - (133\alpha^3/10) + \frac{1144}{35}\alpha^4 + \ldots\right]. \quad (18) $$

For $\alpha \leq 0.2$ terms up to α^3 are sufficient for 5% accuracy.

For $\alpha \gg 1$, Equation (17) becomes

$$ {}_e\sigma \cong \pi r_o^2 \,(1 + 2 \ln 2\alpha) \,/\, 2\alpha \,. \quad (19) $$

Similarly,

$$ {}_e\sigma_s = \pi r_o^2 \left[\frac{\ln(1 + 2\alpha)}{\alpha^3} + \frac{2(1 + \alpha)\,(2\alpha^2 - 2\alpha - 1)}{\alpha^2(1 + 2\alpha)^2} + \frac{8\alpha^2}{3(1 + 2\alpha)^3}\right]. \quad (20) $$

From these, one may obtain the average energy per scattered photon, $(h\nu')_{av}$, as the energy scattered in all collisions divided by the number of collisions; i.e.,

$$ (h\nu')_{av} = (h\nu_o)\; {}_e\sigma_s / {}_e\sigma \,. \quad (21) $$

Using Equations (21) and (4), one obatins the average energy of the recoil electrons, E_{av}.

Also, one may write, using Equations (12), (13), and (2), the number of photons scattered into $dh\nu'$ at $h\nu'$ as

$$ \frac{d({}_e\sigma)}{d\, h\nu'} = \frac{d({}_e\sigma)}{d\Omega}\;\frac{d\Omega}{d\theta}\;\frac{d\theta}{dh\nu'} $$

$$= (\pi r_o^2/\alpha^2 m_o c^2) \left\{ 2 + \left(\frac{h\nu_o - h\nu'}{h\nu'}\right)^2 \left[\frac{1}{\alpha^2} + \frac{h\nu'}{h\nu_o} - \frac{2}{\alpha}\left(\frac{h\nu'}{h\nu_o - h\nu'}\right)\right]\right\} \quad (22)$$

or in terms of α,

$$d({}_e\sigma)/d\alpha' = (\pi r_o^2/\alpha^2) \left\{ (\alpha/\alpha') + (\alpha'/\alpha) - 2[(1/\alpha') - (1/\alpha)] + [(1/\alpha) - (1/\alpha)]^2 \right\} \quad (22)$$

which is plotted in Figure (9).

Various cross sections per electron and average energies are listed below in Table I.

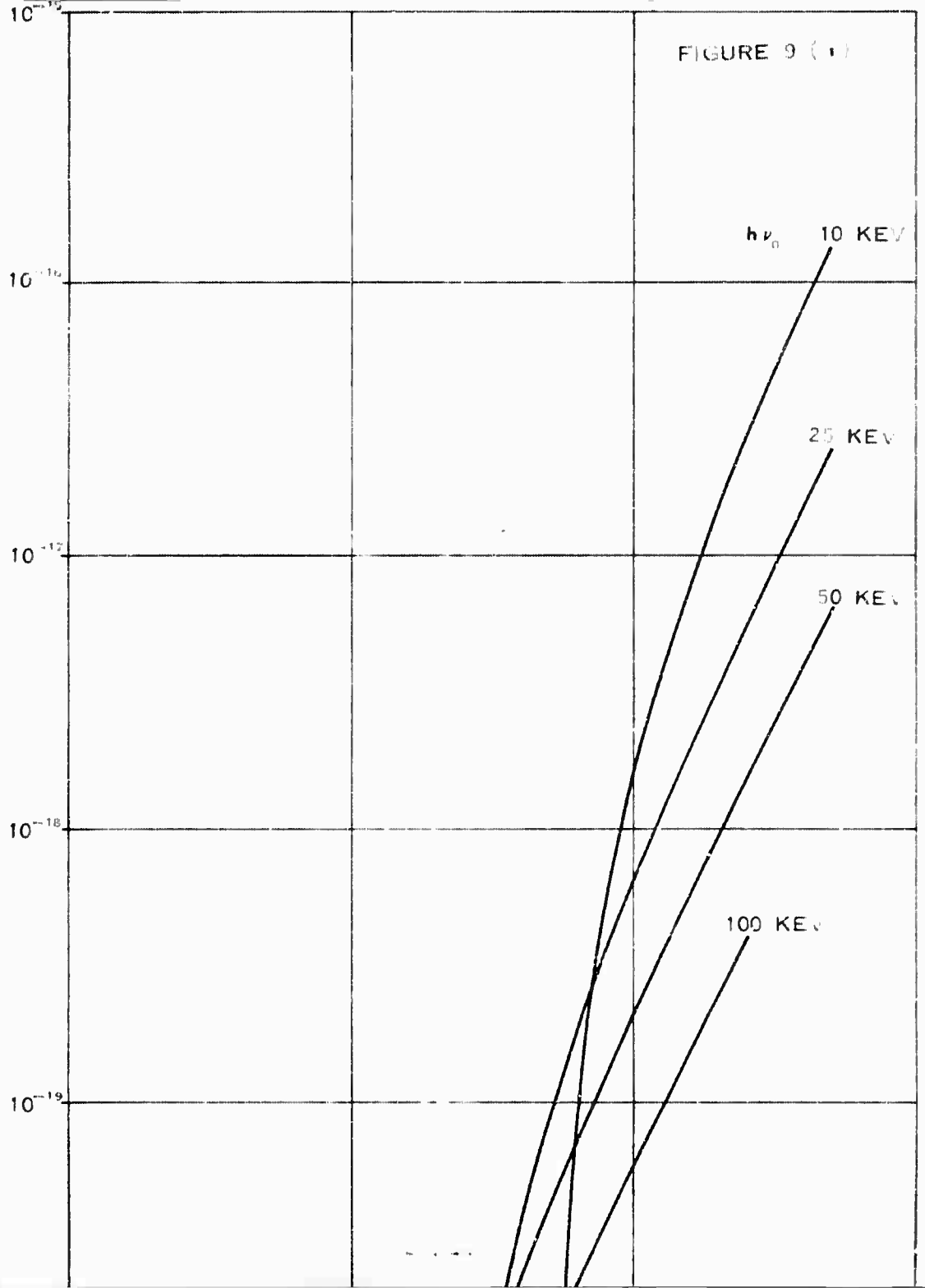
FIGURE 9 ( )
$h\nu_0$ 10 KEV
25 KEV
50 KEV
100 KEV
10^{-18}
10^{-19}
$d\sigma/d\alpha'] = cm^2/$ ELECTRON

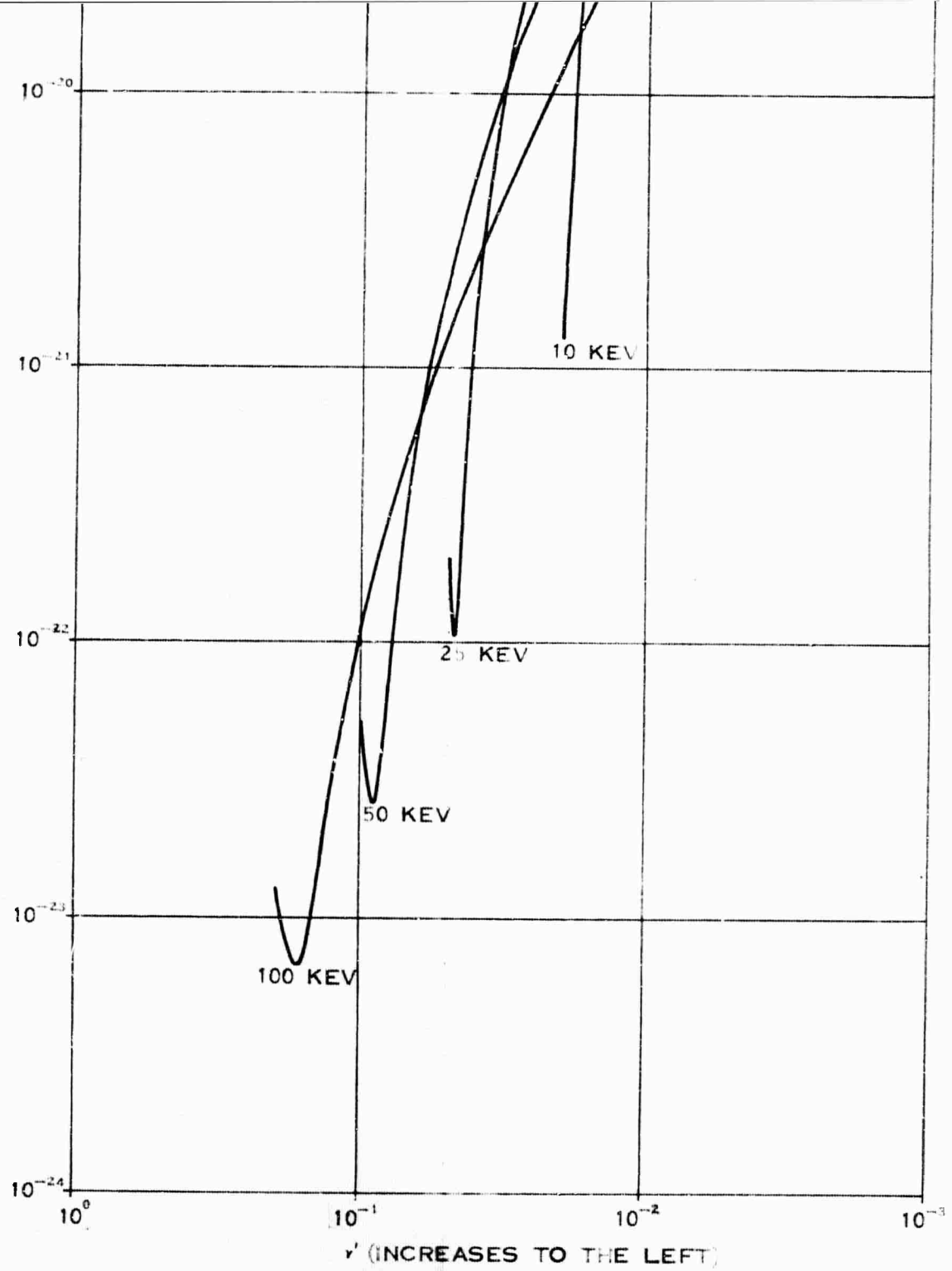
10^{-20}
10^{-21}
10^{-22}
10^{-23}
10^{-24}
10 KEV
25 KEV
50 KEV
100 KEV
10^{0}
10^{-1}
10^{-2}
10^{-3}
ν' (INCREASES TO THE LEFT)

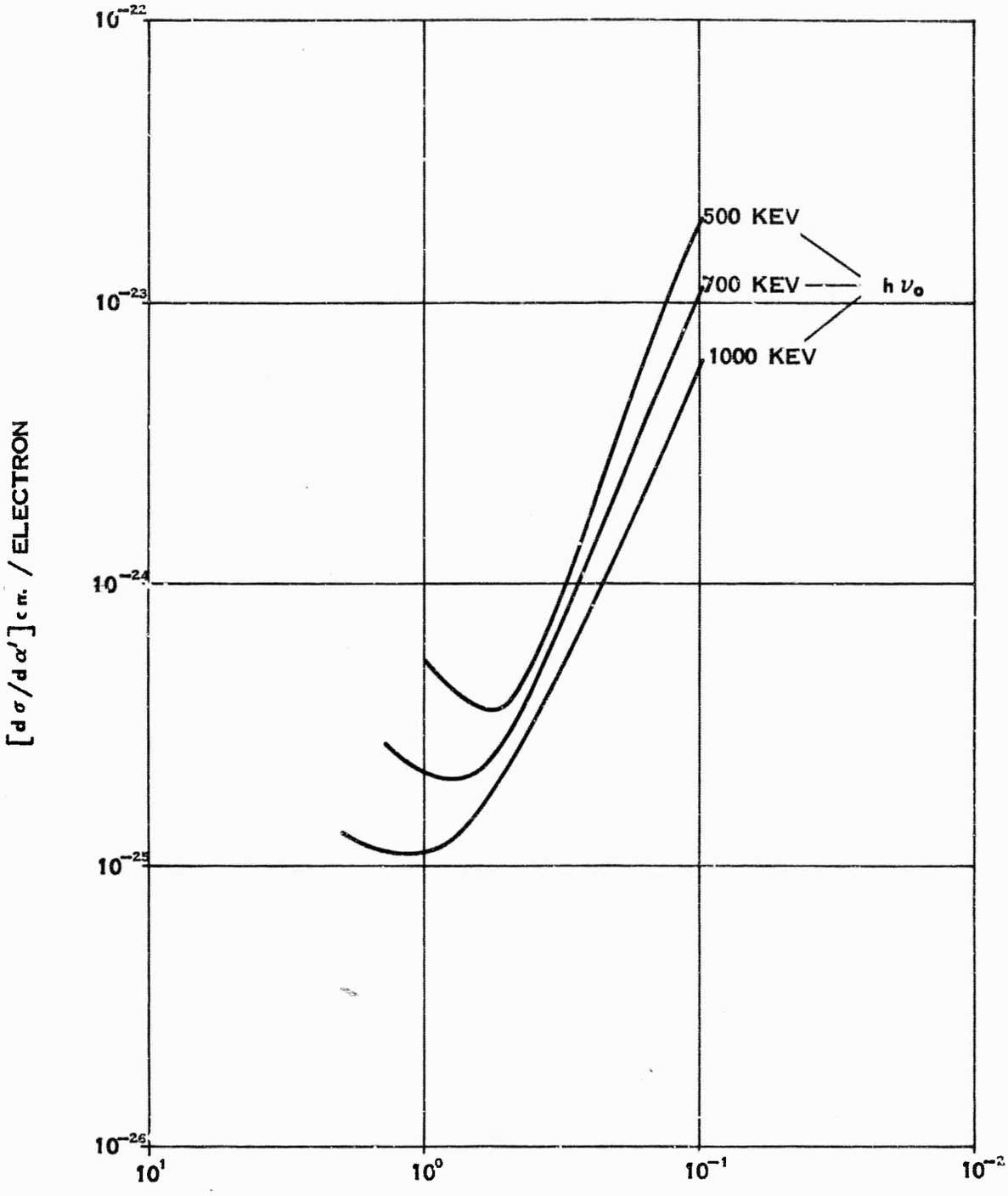
10^{-22}
10^{-23}
10^{-24}
10^{-25}
10^{-26}
500 KEV
700 KEV
1000 KEV
$h\nu_o$
$[d\sigma/d\alpha']_{cm.}$ / ELECTRON
10^{1}
10^{0}
10^{-1}
10^{-2}
α' (INCREASES TO THE LEFT)

FIGURE 9 (b)

Table I

FREE ELECTRON KLEIN-NISHINA AND
RAYLEIGH CROSS SECTIONS AND
AVERAGE ENERGIES

(kev) $h\nu_o$	(10^{-27} cm^2/electron) $_e\sigma$	$_e\sigma_s$	$_e\sigma_a$	(10^{-27} cm^2/electron) σ_R	(kev) $(h\nu')_{av}$	(kev) E_{av}
10	640.5	628.5	12.0	910.	9.8	0.20
15	629.0	611.6	17.4	476.	14.6	0.40
20	618.0	595.7	22.3	303.	19.3	0.70
30	597.6	566.5	31.1	125.	28.4	1.60
40	578.7	540.1	38.6	74.6	37.3	2.70
50	561.5	516.2	45.3	38.0	46.0	4.00
60	545.7	494.5	51.2	28.5	54.4	5.60
80	517.3	456.7	60.6	19.0	70.6	9.40
100	492.8	424.8	68.0	16.3	86.2	13.8
150	443.6	363.1	80.5		122.8	27.2
200	406.5	318.6	87.9		156.8	43.2
300	353.5	258.2	95.3		219.1	80.9
400	316.7	218.6	98.1		276.0	124.
500	289.7	190.5	99.2		329.0	171.
600	267.5	169.2	98.3		379.0	221.
800	235.0	138.9	96.1		473.0	327.
1000	211.2	118.3	92.9		560.0	440.

4. Compton Bound Electron Inelastic Scattering

From Table I, we see that for low $h\nu_o$ the average electron recoil energy becomes of the order of B_e, and the free electron assumption of the Compton effect derivation may be violated. This and the initial momentum an electron has in an atom results in a small shift of $h\nu'$ and $(\lambda' - \lambda_o)$ which we will neglect. More importantly, electron binding affects the differential collision cross section because it introduces a probability that the electron will not be recoiled from the atom but excited to a different bound energy level instead. The mutually independent probabilities of collision, and either recoil or excitation results in a total differential incoherent collision cross section given by

$$d({}_e\sigma_{incoh}) / d\Omega = [d({}_e\sigma) / d\Omega] S \qquad (23)$$

where $S = S(h\nu_o, Z, \theta)$ is the incoherent scattering function[5,6] which may be expressed[7] as a function of a parameter v where

$$v = (2/3)\ (137/Z^{2/3})\ (\alpha)\ \sin(\theta/2) = (4\pi/3)(\alpha_o/\lambda)(1/Z^{2/3})\sin(\theta/2). \qquad (24)$$

Of the various approaches to an analytical expression for S, we select here that derived[5,6] on the Thomas-Fermi atomic model plotted in Figure 10 and given by the empirical equation

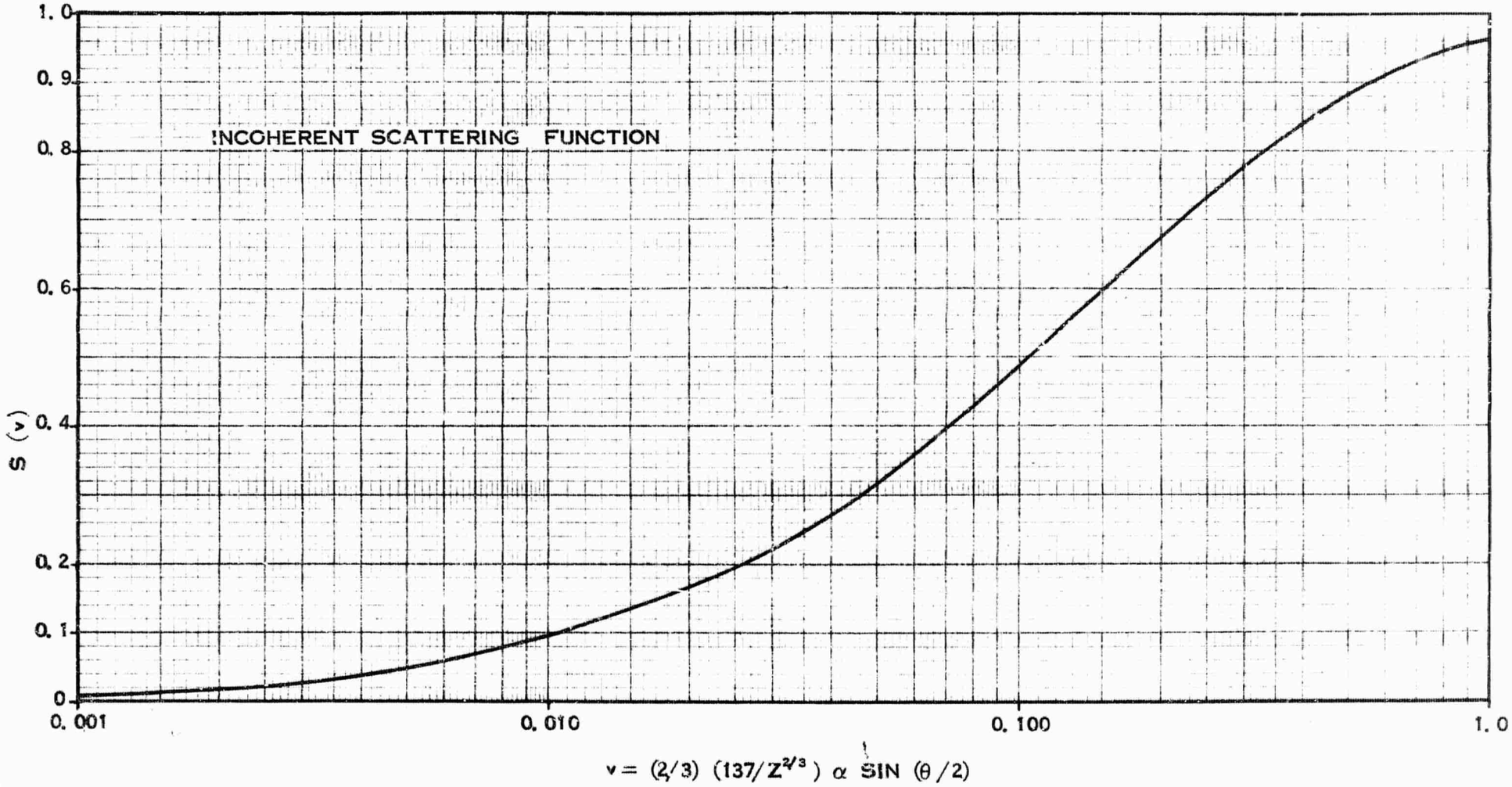
INCOHERENT SCATTERING FUNCTION
1.0
0.9
0.8
0.6
0.4
0.2
0.1
0
S (ν)
0.001
0.010
0.100
1.0
ν = (2/3) (137/Z^2/3) α SIN (θ/2)

FIGURE 10

$$S = 1 - e^{-4.875v^{0.8559}} \qquad (25)$$

to within 10% accuracy.

5. Rayleigh Elastic Scattering

For sufficiently small incident photon energy compared to the electron's binding energy there is too little energy transferred to the electron to produce recoil or excitation. The entire atom absorbs the photon momentum and the scattered radiation has no wavelength shift. All electrons in an atom act similarly so scattering from electrons in the same atom is in phase or coherent and in the low energy limit becomes classical Thomson scattering[8]. (If many atoms are in an ordered arrangement, the scattering is called Bragg reflection.) This may be treated like Compton bound electron scattering by modifying the Thomson differential coherent scattering (no absorption) cross section by an atomic structure factor[9, 10], F, getting

$$d({}_a\sigma_{coh})/d\Omega = (r_o^2/2)\,(1 + \cos^2\theta)\,F^2\,, \qquad (26)$$

where $F = F(h\nu_o, Z, \theta) = F(u)$ and

$$u = 2(137/Z^{1/3})\,\alpha \sin(\theta/2) = 4\pi(a_o/\lambda)(1/Z^{1/3})\sin(\theta/2). \qquad (27)$$

Figure 11 shows F/Z taken from Nelms and Oppenheim[11], from which the empirical expression

$$F/Z = e^{-1.488u^{0.3884}}(1 + u^{-0.2998}) + 3.266 \times 10^{-3} \quad (28)$$

has been computed accurate to within 10%.

6. Photon Transport, Build-Up, and Distribution

Transport through a medium may result in an accumulation of primary direct photons and secondary scattered photons at a point of interest. The ratio of the number of primary plus secondary photons to the number of primary photons at a point is called the build-up factor B.

Upon Compton scattering, the scattered photon has lower energy and is more susceptible to further "energy loss" by additional Compton scattering or photoelectric absorption. A Rayleigh scattered photon has a large probability of being Compton scattered or photoelectrically absorbed upon further collision. An increase in the probability of collisions by an increase in dimension or density of the transport material, therefore, degrades the energy spectrum to lower values, spreads the time of arrival of photons, distributes the directions of arrival of photons, and changes B.

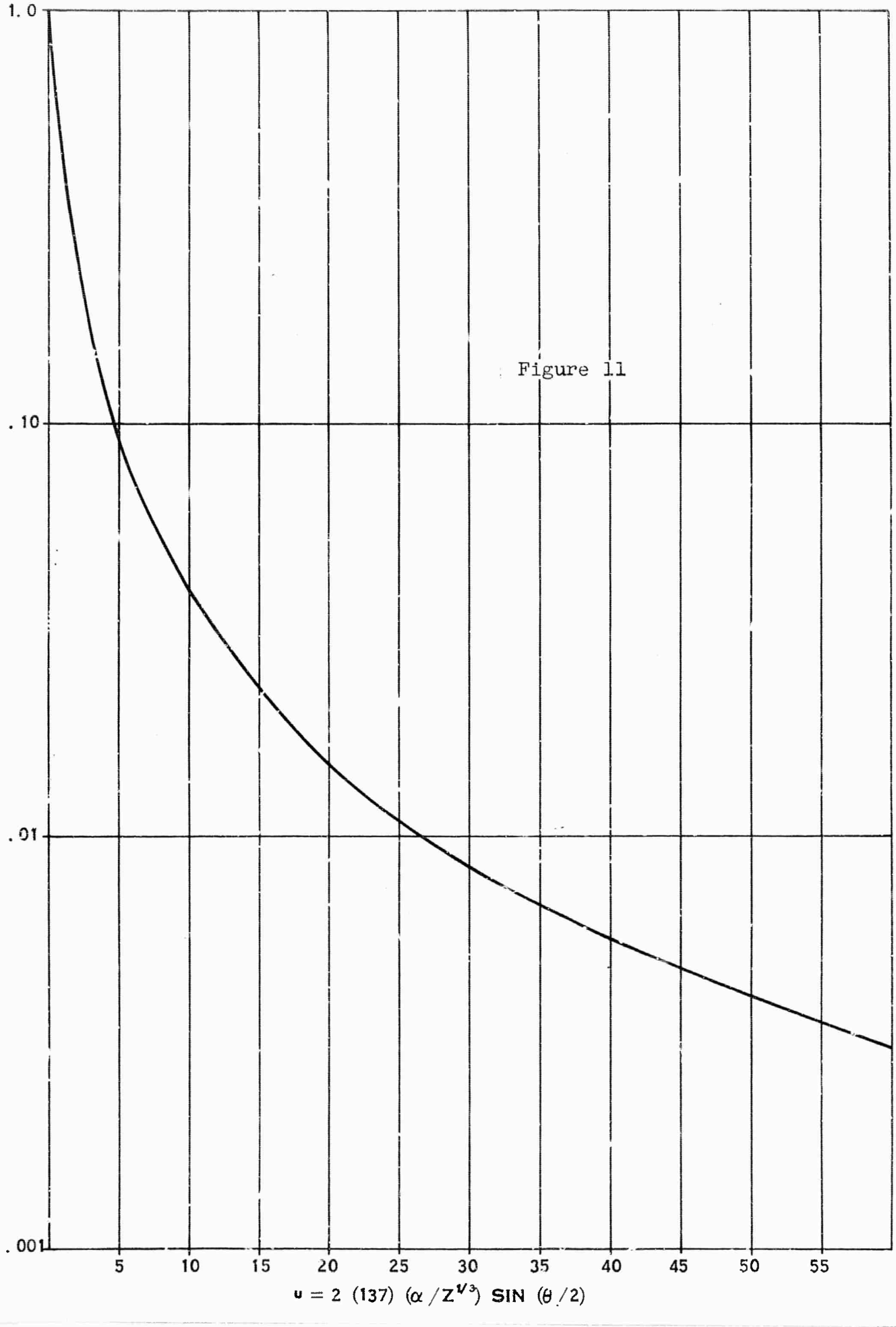
1.0
.10
.01
.001
$\frac{F(u)}{Z}$
5
10
15
20
25
30
35
40
45
50
55
$u = 2\ (137)\ (\alpha / Z^{1/3})\ \text{SIN}\ (\theta / 2)$

Figure 11

If the transport medium geometry (actually distance multiplied by density, ρd) is small compared to photon mean free paths or if only narrow photon beams are considered, then for attenuation the usual exponential expression is used with the attenuation coefficient consisting of $\sigma^{PE} + \sigma^{c} + \sigma^{R}$ with σ^{c} modified for bound electrons[12]. For energy deposition the absorption coefficient $\sigma^{PE} + \sigma_a{}^{c}$ with $\sigma_a{}^{c}$ modified for bound electrons[12] is used. In either case, corrections for fluorescence in high Z materials and Bremsstrahlung at high energies should be considered[13].

When the transport medium ρd is of the order of mean free paths or when the medium has finite thickness but infinite extent so that only a few successive scatterings occur, one may apply the scattering equations the appropriate number of times[14] using the Compton collision or absorption coefficients for attenuation or deposition, respectively. However, if the mean free path of the scattered photon is less than ρd, the probability of its being absorbed before escaping the medium is increased so that for energy deposition the absorption coefficient is only a lower limit while the attenuation coefficient is an upper limit. For ρd much larger than the collision mean free path of the scattered photon, the attenuation coefficient would be used for energy deposition as well as attenuation.

When ρd is sufficiently large for multiple scattering to occur, simple multiple application of the above equations becomes inordinately complicated and solutions to the problem of photon build-up and distribution must be obtained from other methods such as a statistical study of scattering of many photons or the more general transport theory.[14]

Inherent difficulties and inaccuracies in approximate solutions of the general transport theory limit its practical usefulness, therefore, statistical methods such as the Kaman Nuclear Monte Carlo Gamma Ray Transport Code[15] written for the IBM 7090 Computer and recently adapted for x-rays[12] are more popular for practical calculations of photon build-up and distribution resulting from scattering.

A report describing the Monte Carlo computations and including results for air transport, is in preparation.

FOOTNOTES

1. For a comprehensive discussion, see: R. D. Evans, Encyclopedia of Physics, XXXIV, S. Flugge, Editor (Springer-Verlag, Berlin, 1958).

2. Wm. J. Veigele, "Influence of Scattering on X-Ray Transport in Air" (U), Kaman Nuclear, KN-692-64-27(QPR), Chapter 3, Colorado Springs, Colorado, 30 November 1964. SRD.

3. A. H. Compton, Phys. Rev. 21, 207A (1923).

4. O. Klein and Y. Nishina, Z. Physik 52, 853 (1929).

5. W. Heisenberg, Phys. Z. 32, 737 (1931).

6. L. Bewilogua, Phys. Z. 32, 740 (1931).

7. G. R. White, Nat. Bur. of Stds. Report 2763 (1953).

8. J. J. Thomson, Conduction of Electricity Through Gases, 2nd Edition (Cambridge University Press, Cambridge, 1906).

9. A. H. Compton and S. K. Allison, X-Rays in-Theory and Experiment, 2nd Edition (D. Van Nostrand, New York, 1935).

10. J. S. Levinger, Phys. Rev. 87, 656 (1952).

11. Ann T. Nelms and I. Oppenheim, J. Res. Nat. Bur. of Stds. 55, 53 (1955).

12. Wm. J. Veigele, "Influence of Scattering on X-Ray Transport in Air (U)", Kaman Nuclear KN-692-65-28(APR), Chapter 3, Colorado Springs, Colorado, 15 February 1965. SRD.

13. For discussion and tables of modified coefficients, see: J. W. Allison, Austr. J. Res., 14, 443 (1961). A Kaman Nuclear report on fluorescence is in preparation.

14. For a general and comprehensive discussion, see: U. Fano, L. V. Spencer, and M. J. Berger, Encyclopedia of Physics, XXXVIII/2, S. Flugge, Editor (Springer-Verlag, Berlin, 1959).

15. R. E. W. Smith, "Gamma Environment (U)", Kaman Nuclear KN-692-64-24(APR), Chapter 3, Colorado Springs, Colorado, 15 February 1964. SRD.